



1 **Identifying and Quantifying Source Contributions of Air Quality Contaminants**
2 **during Unconventional Shale Gas Extraction**

3 Nur H. Orak^{1,*}, Matthew Reeder^{2,3}, Natalie J. Pekney³

4

5 ¹ *Corresponding author: Tel: +90-216-4140545, nho@alumni.cmu.edu
6 Marmara University, Department of Environmental Engineering

7

8 ² Leidos Research Support Team, National Energy Technology Laboratory,
9 Pittsburgh, PA

10

11 ³U.S. Dept. of Energy National Energy Technology Laboratory, Pittsburgh, PA

12

13

14

15

16

17

18

19

20

21

22

23

24

25

26

27

28

29

30

31

32

33

34

35

36

37

38

39

40

41

42



43 **Abstract**

44 The United States experienced a sharp increase in unconventional natural gas (UNG)
45 development due to the technological development of hydraulic fracturing
46 (“fracking”). The objective of this study is to investigate the effect of unconventional
47 natural gas development activities on local air quality as observed at an active
48 Marcellus Shale well pad at the Marcellus Shale Energy and Environment Laboratory
49 (MSEEL) in Morgantown, Western Virginia, USA. Using an ambient air monitoring
50 laboratory, continuous sampling started in September 2015 during horizontal drilling
51 and ended in February 2016 when wells were in production. High resolution data
52 were collected for the following air quality contaminants: volatile organic compounds
53 (VOCs), ozone (O₃), methane (CH₄), nitrogen oxides (NO and NO₂), carbon dioxide,
54 (CO₂), as well as typical meteorological parameters (wind speed/direction,
55 temperature, relative humidity, and barometric pressure). Positive Matrix
56 Factorization (PMF), a multivariate factor analysis tool, was used to identify possible
57 sources of these pollutants (factor profiles) and determine the contribution of those
58 sources to the air quality at the site. The results of the PMF analysis for well pad
59 development phases indicate that there are three potential factor profiles impacting air
60 quality at the site: *natural gas*, *regional transport/photochemistry*, and *engine*
61 *emissions*. There is a significant contribution of pollutants during horizontal drilling
62 stage to *natural gas* factor. The model outcomes show that there is an increasing
63 contribution to *engine emission* factor over different well pad drilling through
64 production phases. Moreover, model results suggest that the major contributions to
65 the *regional transport/photochemistry* factor occurred during horizontal drilling and
66 drillout stages.

67 Keywords: ambient monitoring; natural gas; air pollution; source apportionment

68



69 **Introduction**

70 There is a rapid increase in unconventional natural gas exploration by recent
71 technological advances (USEIA 2020). The success of the US in exploiting
72 unconventional natural gas has stimulated other countries. As a result, there is a
73 growing attention by public for the potential public health impacts of UNG extraction.
74 In response to emerging public concern regarding the process of fracking for UNG
75 extraction, several studies have investigated the potential public health risks of UNG
76 development (Adgate et al. 2014; Hays et al. 2015; Hays et al. 2017; Werner et al.
77 2015). A part of adverse health effects are related to exposure of environmental
78 pollution (Elliott et al. 2017; Elsner and Hoelzer 2016; Paulik et al. 2016). The
79 majority of environmental impact studies focus on water quality impacts of
80 unconventional natural gas development (Annevelink et al. 2016; Butkovskiy et al.
81 2017; Jackson et al. 2015; Torres et al. 2016). However, relatively fewer studies focus
82 on air quality impacts (Islam et al. 2016; Ren et al. 2019; Swarthout et al. 2015;
83 Williams et al. 2018). Some studies focus on collecting and analyzing data for pre-
84 operational phase of fields to provide baseline dataset for future work that operational
85 shale gas activities can be later evaluated (Purvis et al. 2019). Non-methane
86 hydrocarbons (NMHC) and nitrogen oxides (NO_x) are of most interest as some
87 NMHC can be toxic (such as benzene) (P. M. Edwards et al. 2014), therefore, several
88 studies focuses on increases in methane, NHMC, and ozone in oil and gas producing
89 regions (Pacsi et al. 2015; Roest and Schade 2017). Another study explored the
90 importance of the deployment autonomy of portable measurement systems by
91 measuring exposure upwind, within and downwind of operation of hydraulic
92 fracturing equipment to protect workers (Ezani et al. 2018). There are also more
93 comprehensive studies for data collection. Swarthout et al. (2015) conducted a field
94 campaign to investigate the impact of UNG production operations on regional air
95 quality. Highest density of methane, carbon dioxide, and volatile organic carbons



96 (VOCs) were observed closer to UNG wells. A limited number of studies available on
97 source apportionment for major air pollutants (Majid et al. 2017; Prenni et al. 2016).
98 These studies have lacked a comparison of the effects during distinct operational
99 phases of natural gas extraction: well pad construction, drilling (vertical and
100 horizontal), well stimulation (hydraulic fracturing followed by flowback), and
101 production.

102 Several compounds are associated with emissions from each phase of well installation
103 and development, depending on the activity and equipment in use for each phase.

104 Activities that require the use of off-road diesel construction vehicles have emissions
105 of coarse particulate matter (PM_{10} aerodynamic diameter $\leq 10 \mu m$) from the
106 suspension of dust from vehicle traffic on dirt and gravel roads, as well as volatile
107 organic compounds (VOCs), nitrogen oxides (NO_x) and fine particulate matter
108 smaller than $2.5 \mu m$ in aerodynamic diameter ($PM_{2.5}$) from the vehicle exhaust.

109 During vertical and horizontal drilling, there are emissions of NO_x , $PM_{2.5}$, and VOCs
110 from diesel powered drilling rigs, and fugitive emissions of natural gas (methane
111 (CH_4) and other hydrocarbons). Hydraulic fracturing activities add emissions from
112 truck traffic and diesel-powered compressors (NO_x , PM_{10} , $PM_{2.5}$, VOCs). Emissions
113 of VOCs and CH_4 from water separation tanks, venting, and degassing of produced
114 waters occur during flowback operations. In addition to these primary sources of
115 emissions at the site, secondary production of ozone (O_3) and $PM_{2.5}$ from
116 photochemistry can result from emissions during any of the operational phases.

117 This is the first study, to our knowledge, to collect high time resolution ambient
118 concentrations of compounds emitted from well pad activity during various phases of
119 operation such that the relative air quality effect of each phase of development can be
120 investigated. This detailed information about the distribution of emission sources'



121 impact through a well pad's development phases is needed to manage the associated
122 risks from emissions.

123 **Methods**

124 **Monitoring Location: Marcellus Shale Energy and Environment Laboratory**

125 The Marcellus Shale formation covers an area of approximately 240,000 km² across
126 several states: New York, Pennsylvania, Ohio, West Virginia, Maryland, and
127 Virginia (Kargbo et al. 2010)(Figure S1). The Marcellus Shale Energy and
128 Environment Laboratory (MSEEL) is an approximately 14,000 m² study well pad in
129 Morgantown, WV, USA (39.602° N, 79.976° W) (MSEEL 2019). The MSEEL is a
130 multi-institutional, long-term collaborative field site where integrated geoscience,
131 engineering, and environmental research have been conducted to assess
132 environmental impacts and develop new technology to improve recovery efficiency as
133 well as reduce environmental footprint of shale gas operations (MSEEL 2019).

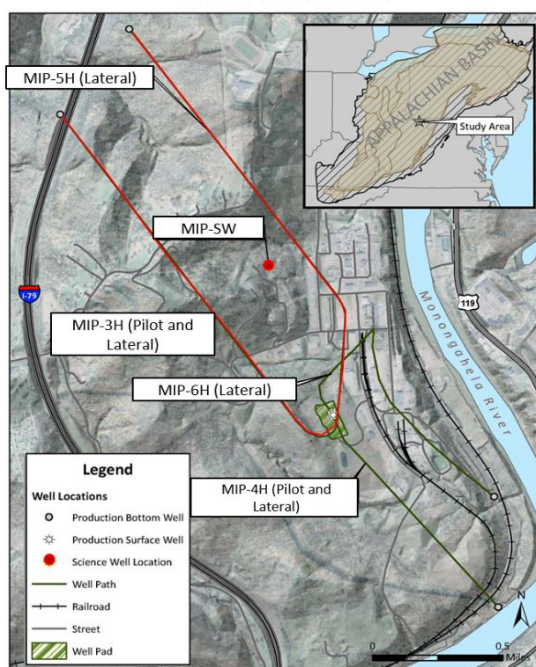


Figure 1. Location of the Marcellus Shale Energy and Environment Laboratory and the four production wells.



134 The MSEEL is the site of two horizontal production wells completed in 2011 (wells
135 4H and 6H, Figure 1) and two horizontal production wells completed in 2015 (wells
136 3H and 5H, Figure 1). Production from the newer horizontal wells began in
137 December 2015. Dates and duration for phases of operation are shown in Figure S2.
138 The vertical drilling was conducted using three diesel Caterpillar 3512 engines with
139 1365 kW generators. Horizontal drilling made use of two dual fuel (40% diesel and
140 60% natural gas) engines. All activities at the well pad followed industry's best
141 management practices (MSEEL 2019).

142 **Air Quality and Meteorological Data Collection**

143 An ambient air monitoring laboratory (18' trailer with ambient air sampled from inlets
144 on the trailer roof) was situated at the northeastern corner of the MSEEL well pad
145 (Figure 1). With wind direction at this location most frequently from the southwest
146 (Figure 2), this position optimized the occurrences of the laboratory being downwind
147 of the well pad. Instrumentation in the laboratory and measured constituents are listed
148 in Table 1. All instruments were maintained and calibrated according to
149 manufacturer's recommended protocols. Details of the laboratory assembly and
150 operation have been previously described (Pekney et al. 2014).

151 Data collected at the air monitoring site is classified by activity at the well pad.
152 Horizontal drilling occurred September 8 – October 5, 2015, first at well 5H then at
153 well 3H. Hydraulic fracturing occurred October 10 – November 16. Cleanout
154 activities followed on November 20-26, which involved using a diesel-powered coil
155 tubing rig to drill out plugs and flush out residue left in the wells.



156

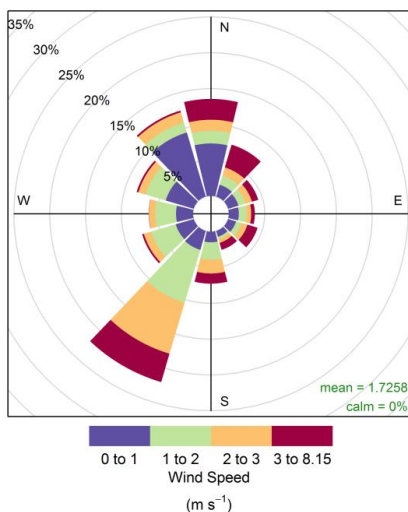


Figure 2. Wind speed and direction during ambient air monitoring campaign at MSEEL (September 2015-February 2016).

157 Flowback, the flowing of gas, formation fluid, and frac fluid up the wells to the
158 surface, took place over December 10-14, after which both wells were in production.
159 A reduced emission completion (REC) was performed; gas produced during this time
160 was captured using portable equipment brought on site that separates the gas from the
161 liquids so that the gas can be retained as a product.

162 Air monitoring began September 18, 2015 and ended February 1, 2016. No data were
163 collected for the vertical drilling phase. Data collection was continuous except for
164 calibration and instrument downtime. The laboratory's meteorological station
165 measured relative humidity, temperature, rainfall, solar radiation, wind direction,
166 wind speed, and barometric pressure at an elevation of 10m.

167

168

169

170



171 Table 1. Constituents measured by the MSEEL mobile air monitoring laboratory
 172 (Pekney et al. 2018).

Measurement	Unit	Resolution	Sampling Rate	Instrument	Measurement technique
VOCs (52 compounds, see Table S1 for full list)	ppb	0.4 ppb	1 hour	Perkin Elmer Ozone Precursor Analyzer (Waltham, Massachusetts)	Gas Chromatograph with Flame Ionization Detection (GC—FID) with thermal desorption
Ozone, NO _x	ppb	0.4 ppb Ozone, 50 ppb NO _x	1 minute	Teledyne-API Gas Analyzers T400 and T200U (San Diego, California)	UV absorption, Chemiluminescence
Methane, carbon dioxide	ppm	<5 ppb Methane, 1 ppm CO ₂	1 second	Picarro G2201-i (Santa Clara, California)	Cavity Ring-Down Spectrometry
Meteorological Parameters: wind speed and direction, temperature, relative humidity, barometric pressure, rainfall, and solar intensity	various	Various; 1 degree for wind direction/ 0.45 m/s for wind speed for Vantage Pro2 Plus; 0.1 degree for wind direction/ 0.01 m/s wind speed for R.M. Young 81000	1 minute	Davis Instruments Vantage Pro2 Plus (Oakland, California) and R.M. Young 81000 ultrasonic anemometer (Traverse City, Michigan)	Various

173 **Source-Receptor Modeling**

174 Positive Matrix Factorization (PMF), a factor analysis method (Figure S3), was
 175 applied to hourly averaged ambient concentrations of measured species to identify
 176 possible sources and patterns for the stages of development. PMF decomposes the
 177 sample data into two matrices: factor profiles (representative of *sources*) and factor
 178 contributions (Brown et al. 2015; Norris et al. 2014). The fundamental objective of
 179 PMF is to solve the chemical mass balance (Equation 1) between measured species
 180 concentrations and source profiles while optimizing goodness of fit (Equation 2):



181 Mass balance (Evans and Jeong 2007):

$$182 \quad x_{i,j} = \sum_{k=1}^p g_{ik} f_{kj} + e_{ij}$$

183 [1]

184 where $x_{i,j}$ is the data matrix with dimensions of i (observations) by j (chemical
185 species), p is the optimum number of factors, g_{ik} is the factor contribution to the
186 observation, f_{kj} is the species profile of the factor, k is the factor, and $e_{i,j}$ is the residual
187 concentration for each observation.

188 Goodness of fit:

$$189 \quad Q = \sum_{i=1}^n \sum_{j=1}^m \left(\frac{x_{ij} - \sum_{k=1}^p g_{ik} f_{kj}}{s_{ij}} \right)^2$$

190 [2]

191 where Q is the goodness of fit, n is the total number of observations, m is the total
192 number of chemical species, and s_{ij} is the uncertainty for each observation. Summary
193 of methods for uncertainty calculations are provided in Supplemental Information.
194 Missing values within the data set are replaced with the median value of that species;
195 also, uncertainty for missing values is set at four times the species-specific median by
196 the program. Multiple runs with different numbers of factors are executed for each
197 data set. The output of the PMF analysis needs to be interpreted by the user to identify
198 the number of factors that may be contributing to the samples and the possible sources
199 they represent. One of the main strengths of PMF analysis is that each sample is
200 weighted individually, which allows the user to adjust the influence of each sample
201 based on the measurement confidence.

202 Signal-to-noise ratio (S/N), an indicator of the accuracy of the variability in the
203 measurements, can be used to identify a species as “Strong”, “Weak”, or “Bad”.



204 Generally, if this ratio is greater than 0.5 but less than 1 that species has a “Weak”
205 signal. “Strong” is the default value for all species with an assumption of S/N greater
206 than 1. “Bad” category excludes the species from the rest of the analysis. We
207 considered the number of samples that are missing or below the detection limit when
208 choosing the category for each species. (Norris et al. 2014). The expected goodness
209 of fit (Q_{expected}) is calculated for each scenario (Norris *et al.*, 2014):

210 Expected goodness of fit:

$$211 \quad Q_{\text{expected}} = (i \times j) - \{(p \times i) + (p \times j)\}$$

212 [3]

213 where $(i \times j)$ is the number of non-weak data values in X_{ij} and $(p \times i)$ and $(p \times j)$ are
214 the number of elements in G and F, respectively. Q_{robust} is the calculated goodness-of-
215 fit parameter that excludes points that are not fit by the model. The lowest
216 $Q_{\text{robust}}/Q_{\text{expected}}$ is calculated to compare different factor scenarios; when changes in Q
217 become small with increasing factors, it can indicate that there may be too many
218 factors in the solution (Brown et al. 2015).

219 In addition to these calculated parameters, factor profiles and error estimation
220 diagnostics are used to compare the output of different simulations. Marker species
221 (chemical species that are unique to a particular source) and temporal or seasonal
222 variations can be used to aid in identifying the possible emission sources (Figure 3).
223 Associations between factors can also provide useful information for profile
224 characterization. Moreover, meteorological data can provide useful information about
225 the geographic location of the sources.

226 In order to perform the PMF analysis, we utilized a user-friendly graphical user
227 interface (GUI) developed by the U.S. Environmental Protection Agency (EPA), EPA
228 PMF 5.0 (Norris et al., 2014). Hourly average data was used for each pollutant to



229 unify the measurement intervals. All pollutants included in the matrix were identified
230 as “strong” (signal to noise: $S/N > 2$). Fifty base runs were performed, and the run
231 with the minimum Q value was selected as the base run solution. In each case, the
232 model was run in the robust mode with a number of repeat runs to ensure the model
233 least-squares solution represents a global rather than a local minimum. First, the
234 rotational (linear transformation) Fpeak variable was held at the default value of 0.0.
235 However, there can be almost infinite possibilities of F and G matrices that produces
236 the same minimum Q value, but the goal is producing a unique solution. As a result,
237 rotational freedom is one of the main sources of uncertainty in PMF solutions
238 (Paatero et al. 2014). Therefore, Fpeak values were adjusted (-1.0, -0.5, 0.5, and 1.0)
239 to explore how much rotational ambiguity exists in PMF solutions. In other words, the
240 model adds and/or subtracts rows and columns of F and G matrices based on the
241 Fpeak value, which is typically between -5 and +5 (Norris et al. 2014). Positive Fpeak
242 values cause a sharpened F-matrix and smeared G-matrix; negative Fpeak values
243 result in subtractions in the G-matrix. The factor contributions were analyzed to find
244 the optimum Fpeak value.

245 The PMF analysis was completed with error estimation. We used three methods of
246 error estimation: Bootstrap (BS), Displacement (DISP), and BS-DISP, which guide
247 understanding the stability of the PMF solution (Norris et al. 2014). BS analysis is
248 used to determine whether a set of observations affect the solution disproportionately.
249 The main idea of BS analysis is resampling different versions of the original data set
250 and perform PMF analysis. Random errors and rotational ambiguity affect BS error
251 intervals. The main reason of rotational ambiguity is the existence of infinite solutions
252 similar to the solution generated by PMF solution. DISP analysis helps to analyze the
253 PMF solution in detail. Only rotational ambiguity affects DISP error intervals.
254 BS-DISP is a hybrid method that gives more robust results than DISP results.



255 Results and Discussion

256 Overview of Results for Measured Compounds

257 Figure 3 shows a box-and-whisker graph of the measured NO_x, NO, NO₂, Ozone, and
258 ethane during the whole monitoring campaign at the study site. Similarly, Figure 4
259 shows a statistical summary of methane and carbon dioxide. The y-axis represents
260 concentrations and the x-axis represents the phases of the well development. The
261 black line on each of the boxes represents the median for that particular data set. The
262 small circles represent outliers. The blue circles represent the mean. Since most of the
263 VOCs concentrations measured were consistently below 10 ppb, only ethane is
264 included. There was an increase for NO_x (25th percentile (q1)=12.5 ppb) and NO (q
265 1= 2.7 ppb) during the *fracturing* phase compared to other phases. The whiskers show
266 the high variability for this phase, which can be a result of small sample size for the
267 *fracturing* phase. NO/NO₂ ratio for 25th and 75th percentiles was 1.2, indicating
268 fresher, less oxidized emissions. The skewness of the data for this phase indicates that
269 the data may not be normally distributed. NO₂ graph shows a similar trend for the
270 *fracturing* phase. We did not observe significant differences for different development
271 phases for ozone, which is not surprising as it is a secondary pollutant and it can be
272 related to winter season of the data collection period. (Peter M. Edwards et al. 2014).
273 There was a dramatic increase for the flowback phase for ethane concentration. This
274 25th percentile was 24 ppb, while this concentration ranged between 0 and 11 ppb for
275 other phases. The 75th percentile was 89 ppb, which is a significantly higher value
276 compared to other phases. We observed a similar trend for methane concentration.
277 The 25th percentile (2.5 ppm) and the 75th percentile (4.3 ppm) were significantly
278 higher than other phases. Differences for development phases for CO₂ were not
279 statistically significantly different. CO₂ has many emissions sources and variable



280 background concentrations so distinguishing emissions from the well pad activities is
281 difficult.

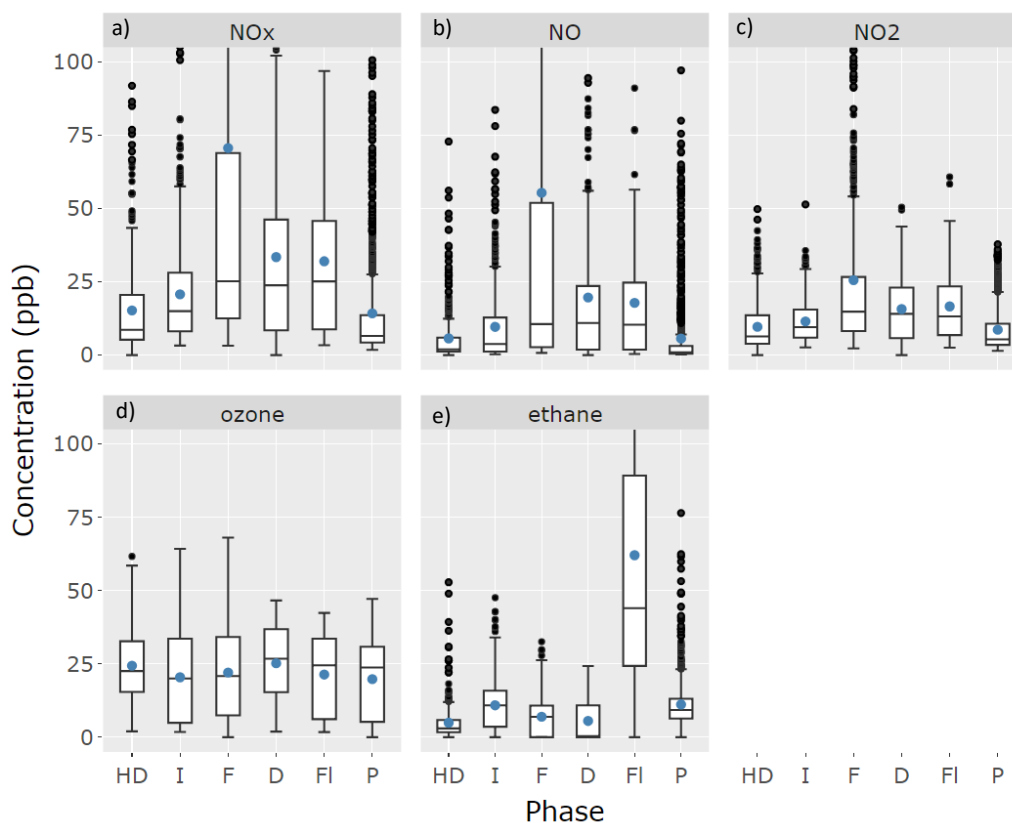


Figure 3. Summary statistics of input parameters for (a) NO_x , (b) NO , (c) NO_2 , (d) Ozone, (e) ethane (HD: Horizontal Drilling, I: Idle, F: Fracturing, D: Drillout, FI: Flowback, P: Production. The idle phase consists of gaps of time between other operational phases, when there was little to no emissions-generating activity on the well pad.

282 The average concentrations of methane and ethane for the entire monitoring campaign
283 are shown in Figure S4. The highest ethane concentrations occurred during the
284 *flowback* stage (565.7 ppb). A mean that is significantly higher than the median
285 comes from a distribution that is skewed due to peak events ($\text{mean}_{\text{ethane}} = 11.4$ ppb,
286 $\text{median}_{\text{ethane}} = 8.5$ ppb). Propane and isobutane had the second and third highest
287 average concentrations, respectively, for each phase of development. Similarly, the



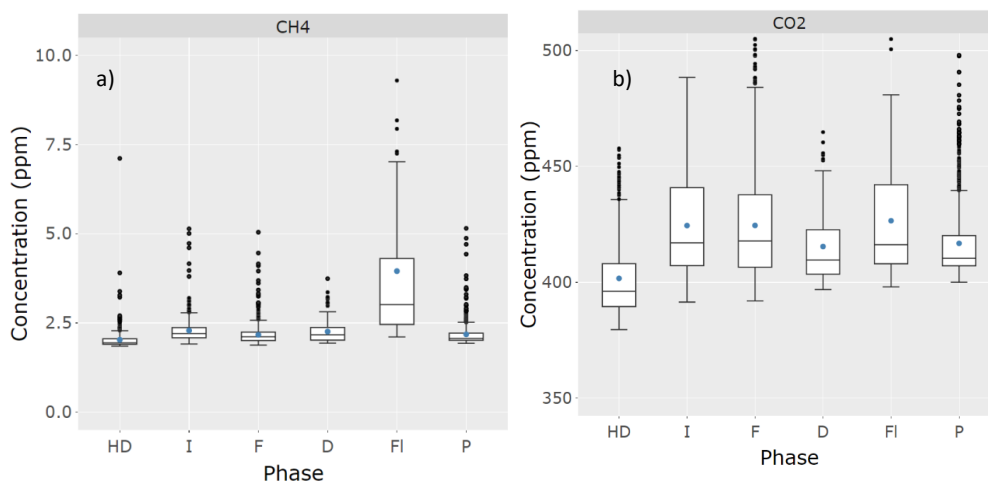
288 hourly concentration graphs of NO_x, O₃, and CH₄, and CO₂ were used to analyze the
289 factor solutions (Figure S5).

290 **Factor Profiles**

291 The three-factor model was chosen for the PMF analysis based on the interpretation
292 of the factor profiles, $Q_{\text{robust}}/Q_{\text{expected}}$ ratios, factor contributions, error estimation
293 results, and hourly peak concentrations of pollutants (Figure S6). The three-factor
294 solution was resolved to the following factors: *natural gas* for the natural gas-related
295 emissions sources; *regional transport/photochemistry* for the atmospheric regional
296 molecular transport and oxidized background air; and *engine emissions* for emissions
297 from vehicles, drill rigs, generators, and pumps used at the site (Figure 5). The
298 summary of PMF models with various F_{peak} values for well development activities
299 are shown in Table S4. The DISP, BS, and BS-DISP results for 2, 3, and 4 factor PMF
300 solutions are summarized in Table S2. For the 3-factor analysis, the DISP results
301 indicate that there are no swaps and the PMF solution is stable, which means there are
302 no exchange factor identities and it is a well-defined solution for the case. According
303 to BS results, there is a small uncertainty; this can be an impact of high variability in
304 concentration. BS-DISP captures both random errors and rotational ambiguity; these
305 results also indicate that the solution is reliable because there are no swaps between
306 factors for the PMF model. Error estimation summary plots (Figure S6) show range of
307 concentration by species in each factor: Base Value, BS 5th, BS Median, BS 95th,
308 BS-DISP 5th, BS-DISP Average, BS-DISP 95th, DISP Min, DISP Average, and DISP
309 Max.

310

311



312 Figure 4. Summary statistics of input parameters for methane (a) and carbon dioxide
313 for (b) (HD: Horizontal Drilling, I: Idle, F: Fracturing, D: Drillout, FI: Flowback, P:
314 Production.

315 Source Profiles

316 **The natural gas factor** was named as such due to its composition of species that are
317 present in natural gas: 1% methane, 3% ethane, 1.5% propane, 0.5% isobutane, 1% n-
318 butane, 0.1% pentane, and 0.2% isopentane. Ethane is a particularly good marker for
319 natural gas emissions sources due because its atmospheric sources are almost
320 exclusively from natural gas extraction, production, processing and use (Liao et al.
321 2017). Ninety-two percent of ethane mass is explained by the natural gas factor. The
322 highest contribution for this factor occurred during the flowback phase.

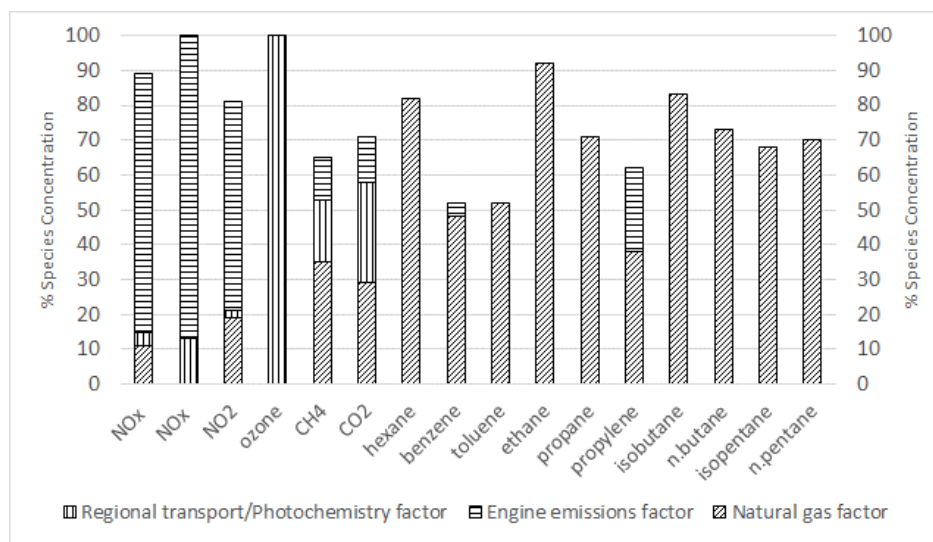
323 **The regional transport/photochemistry factor** was characterized by high
324 contributions from ozone (12%), CH₄ (1%), and CO₂ (86%). Ninety-nine percent of
325 the ozone mass was explained by this factor. Ozone is a product of photochemistry
326 and not directly emitted by any of the sources on the well pad. Although CH₄ and
327 CO₂ would be emitted by well pad sources, they are also present in background
328 ambient air and could be transported to the monitoring location from other sources in



329 the region. Contributions of this factor were relatively steady for all phases of
330 operation during the entire monitoring campaign.

331 **The engine emissions factor** was composed of 39% NO_x, 33% NO, and 11% NO₂ as
332 well as 0.02% toluene and 0.04% benzene. The portions of the mass of these species
333 explained by this factor are 74%, 87%, 60%, 20%, and 54%, respectively. Toluene is
334 released mainly from motor vehicle emissions and chemical spills (Gierczak et al.
335 2017). Contribution of this factor was significantly highest during hydraulic
336 fracturing, when there were emissions from many diesel engines operating
337 continuously on the well pad. Contribution during flowback was also elevated.
338 Several peaks of contribution were observed during production, which could be due to
339 maintenance vehicles and other short-lived vehicle-based activities on the well pad.

340



341
342 Figure 5. The three-factor solution fingerprints for Drilling through Production
343 Monitoring Period, $F_{\text{peak}}=1$.

344 The main limitation of the study is having uneven number of data points for each
345 operational phase. This limitation affects the analyses; however, we do not have
346 control of the durations of the operational phases. As a future work, integrating more
347 data from different fields can decrease the inherent uncertainty.



348 **Conclusion**

349 We investigated the effect of unconventional natural gas development activities on
350 local air quality by using ambient air monitoring laboratory near Marcellus Shale well
351 pad in Morgantown, Western Virginia. The results of PMF solutions for well pad
352 development phases show that there were three potential factor profiles as outlined in
353 Figure 5: *natural gas*, *regional transport/photochemistry*, and *engine emissions*.
354 Horizontal drilling stage had an important contribution to the *natural gas* factor. In
355 addition, there was a significant concentration contribution at the end of the horizontal
356 drilling phase. An increasing contribution to *engine emission* factor was observed
357 over different well pad drilling through production phases. The peak concentration
358 was observed during the drillout stage. Even though it is difficult to compare the
359 *regional transport/photochemistry* contributions due to high variability, highest
360 contributions occurred during horizontal drilling and drillout.

361 As determined by the PMF analysis, a measurable increase in natural gas-related
362 pollutant concentrations and the associated natural gas factor contribution from
363 different stages of active phase was not observed. At the downwind distance of 600m
364 from the well pad center to the air monitoring laboratory, the emissions from the well
365 pad were not easily distinguishable from typical variations in ambient background
366 concentrations. West Virginia has many natural gas wells that contribute to the
367 ambient background, as evidenced by ethane concentrations that are higher than
368 typical global background (Rinsland et al. 1987; Rudolph et al. 1996). Short-lived
369 peak events that were observed when the wind direction was coming from the well
370 pad show that emissions can be dispersed downwind and detected at this distance, but
371 when concentrations are averaged and analyzed with a PMF analysis the peak events
372 were not significant enough to result in a measurable impact of the well pad emissions
373 at the receptor location. Understanding the air quality impacts of operational phases is



374 important since it has potential to help inform future decision-making and constrain
375 cumulative impact assessments.

376

377 **Conflicts of interest**

378 There are no conflicts to declare.

379 **Acknowledgements**

380 Disclaimer: This report was prepared as an account of work sponsored by an agency
381 of the United States Government. Neither the United States Government nor any
382 agency thereof, nor any of their employees, makes any warranty, express or implied,
383 or assumes any legal liability or responsibility for the accuracy, completeness, or
384 usefulness of any information, apparatus, product, or process disclosed, or represents
385 that its use would not infringe privately owned rights. Reference therein to any
386 specific commercial product, process, or service by trade name, trademark,
387 manufacturer, or otherwise does not necessarily constitute or imply its endorsement,
388 recommendation, or favoring by the United States Government or any agency thereof.
389 The views and opinions of authors expressed therein do not necessarily state or reflect
390 those of the United States Government or any agency thereof.

391 This technical effort was performed in support of the National Energy Technology
392 Laboratory's ongoing research under the Natural Gas Infrastructure Field Work
393 Proposal DOE 1022424. This research was supported in part by appointments to the
394 National Energy Technology Laboratory Research Participation Program, sponsored
395 by the U.S. Department of Energy and administered by the Oak Ridge Institute for
396 Science and Education. Authors would also like to thank James I. Sams III, and
397 Richard W. Hammack.

398 **Author Contribution**



399 **Nur H Orak:** Conceptualization, Methodology, Software. Visualization, Writing
400 **Natalie J. Pekney:** Supervision, Methodology, Writing. **Matthew Reeder:**
401 Methodology, Validation.

402 **Code/Data availability**

403 Model simulations presented in this paper are available upon request.

404 **References**

- 405 Adgate JL, Goldstein BD, McKenzie LM. 2014. Potential public health hazards,
406 exposures and health effects from unconventional natural gas development.
407 *Environmental science & technology* 48:8307-8320.
- 408 Annevelink M, Meesters JAJ, Hendriks AJ. 2016. Environmental contamination due
409 to shale gas development. *The Science of the total environment* 550:431-438.
- 410 Brown SG, Eberly S, Paatero P, Norris GA. 2015. Methods for estimating uncertainty
411 in pmf solutions: Examples with ambient air and water quality data and
412 guidance on reporting pmf results. *Science of the Total Environment* 518-
413 519:626-635.
- 414 Butkovskiy A, Bruning H, Kools SAE, Rijnaarts HHM, Van Wezel AP. 2017.
415 Organic pollutants in shale gas flowback and produced waters: Identification,
416 potential ecological impact, and implications for treatment strategies.
417 *Environmental science & technology* 51:4740-4754.
- 418 Edwards PM, Brown SS, Roberts JM, Ahmadov R, Banta RM, deGouw JA, et al.
419 2014. High winter ozone pollution from carbonyl photolysis in an oil and gas
420 basin. *Nature* 514:351-354.
- 421 Edwards PM, Brown SS, Roberts JM, Ahmadov R, Banta RM, deGouw JA, et al.
422 2014. High winter ozone pollution from carbonyl photolysis in an oil and gas
423 basin. *Nature* 514:351-354.
- 424 Elliott EG, Trinh P, Ma X, Leaderer BP, Ward MH, Deziel NC. 2017.
425 Unconventional oil and gas development and risk of childhood leukemia:
426 Assessing the evidence. *Science of The Total Environment* 576:138-147.
- 427 Elsner M, Hoelzer K. 2016. Quantitative survey and structural classification of
428 hydraulic fracturing chemicals reported in unconventional gas production.
429 *Environmental science & technology* 50:3290-3314.
- 430 Evans GJ, Jeong JH. 2007. Data analysis and source apportionment of pm2.5 in
431 golden, british columbia using positive matrix factorization (pmf). R-WB-
432 2007-02. Environment Canada, The University of Toronto.
- 433 Ezani E, Masey N, Gillespie J, Beattie TK, Shipton ZK, Beverland IJ. 2018.
434 Measurement of diesel combustion-related air pollution downwind of an
435 experimental unconventional natural gas operations site. *Atmospheric*
436 *Environment* 189:30-40.
- 437 Gierczak CA, Kralik LL, Mauti A, Harwell AL, Maricq MM. 2017. Measuring nmhc
438 and nmog emissions from motor vehicles via ftir spectroscopy. *Atmospheric*
439 *Environment* 150:425-433.
- 440 Hays J, Finkel ML, Depledge M, Law A, Shonkoff SBC. 2015. Considerations for the
441 development of shale gas in the united kingdom. *Science of The Total*
442 *Environment* 512-513:36-42.
- 443 Hays J, McCawley M, Shonkoff SB. 2017. Public health implications of
444 environmental noise associated with unconventional oil and gas development.
445 *The Science of the total environment* 580:448-456.
- 446 Islam SMN, Jackson PL, Aherne J. 2016. Ambient nitrogen dioxide and sulfur
447 dioxide concentrations over a region of natural gas production, northeastern
448 british columbia, canada. *Atmospheric Environment* 143:139-151.



- 449 Jackson RB, Lowry ER, Pickle A, Kang M, DiGiulio D, Zhao K. 2015. The depths of
450 hydraulic fracturing and accompanying water use across the united states.
451 Environmental science & technology 49:8969-8976.
- 452 Kargbo DM, Wilhelm RG, Campbell DJ. 2010. Natural gas plays in the marcellus
453 shale: Challenges and potential opportunities. Environmental Science &
454 Technology Feature 44:5679-5684.
- 455 Liao HT, Yau YC, Huang CS, Chen N, Chow JC, Watson JG, et al. 2017. Source
456 apportionment of urban air pollutants using constrained receptor models with a
457 priori profile information. Environmental pollution 227:323-333.
- 458 Majid A, Val Martin M, Lamsal LN, Duncan BN. 2017. A decade of changes in
459 nitrogen oxides over regions of oil and natural gas activity in the united states.
460 Elementa: Science of the Anthropocene 5.
- 461 MSEEL. 2019. Marcellus shale energy and environment laboratory. Available:
462 www.mseel.org.
- 463 Norris G, Duvall R, Brown S, Bai S. 2014. Epa positive matrix factorization (pmf) 5.0
464 fundamentals and user guide. Washington, DC 20460.
- 465 Paatero P, Eberly S, Brown SG, Norris GA. 2014. Methods for estimating uncertainty
466 in factor analytic solutions. Atmospheric Measurement Techniques 7:781-797.
- 467 Pacsi AP, Kimura Y, McGaughey G, McDonald-Buller EC, Allen DT. 2015.
468 Regional ozone impacts of increased natural gas use in the texas power sector
469 and development in the eagle ford shale. Environmental science & technology
470 49:3966-3973.
- 471 Paulik LB, Donald CE, Smith BW, Tidwell LG, Hobbie KA, Kincl L, et al. 2016.
472 Emissions of polycyclic aromatic hydrocarbons from natural gas extraction into
473 air. Environmental science & technology 50:7921-7929.
- 474 Pekney NJ, Veloski G, Reeder M, Tamilia J, Rupp E, Wetzel A. 2014. Measurement
475 of atmospheric pollutants associated with oil and natural gas exploration and
476 production activity in pennsylvania's allegheny national forest. Journal of the
477 Air & Waste Management Association 64:1062-1072.
- 478 Pekney NJ, Reeder MD, Mundia-Howe M. Air quality measurements at the marcellus
479 shale energy and environment laboratory site In: Proceedings of the
480 A&WMA's 111th Annual Conference & Exhibition, 2018. Hartford,
481 Connecticut, USA.
- 482 Prenni AJ, Day DE, Evanoski-Cole AR, Sive BC, Hecobian A, Zhou Y, et al. 2016.
483 Oil and gas impacts on air quality in federal lands in the bakken region: An
484 overview of the bakken air quality study and first results. Atmos Chem Phys
485 16:1401-1416.
- 486 Purvis RM, Lewis AC, Hopkins JR, Wilde SE, Dunmore RE, Allen G, et al. 2019.
487 Effects of 'pre-fracking' operations on ambient air quality at a shale gas
488 exploration site in rural north yorkshire, england. The Science of the total
489 environment 673:445-454.
- 490 Ren X, Hall DL, Vinciguerra T, Benish SE, Stratton PR, Ahn D, et al. 2019. Methane
491 emissions from the marcellus shale in southwestern pennsylvania and northern
492 west virginia based on airborne measurements. Journal of Geophysical
493 Research: Atmospheres 124:1862-1878.
- 494 Rinsland CP, Zander R, Farmer CB, Norton RH, Russell JM. 1987. Concentrations of
495 ethane (c2h6) in the lower stratosphere and upper troposphere and acetylene
496 (c2h2) in the upper troposphere deduced from atmospheric trace molecule
497 spectroscopy/spacelab 3 spectra. . JGR Atmospheres 92.
- 498 Roest G, Schade G. 2017. Quantifying alkane emissions in the eagle ford shale using
499 boundary layer enhancement. Atmos Chem Phys 17:11163-11176.



- 500 Rudolph J, Koppmann R, Plass-Dulmer C. 1996. The budgets of ethane and
501 tetrachloroethane: Is there evidence for an impact of reactions with chlorine
502 atoms in the troposphere? . *Atmospheric Environment* 30:1887-1894.
- 503 Swarthout RF, Russo RS, Zhou Y, Miller BM, Mitchell B, Horsman E, et al. 2015.
504 Impact of marcellus shale natural gas development in southwest pennsylvania
505 on volatile organic compound emissions and regional air quality.
506 *Environmental science & technology* 49:3175-3184.
- 507 Torres L, Yadav OP, Khan E. 2016. A review on risk assessment techniques for
508 hydraulic fracturing water and produced water management implemented in
509 onshore unconventional oil and gas production. *The Science of the total
510 environment* 539:478-493.
- 511 USEIA. 2020. Shale gas production. Available:
512 https://www.eia.gov/dnav/ng/ng_prod_shalegas_s1_a.htm [accessed June 10,
513 2020].
- 514 Werner AK, Vink S, Watt K, Jagals P. 2015. Environmental health impacts of
515 unconventional natural gas development: A review of the current strength of
516 evidence. *The Science of the total environment* 505:1127-1141.
- 517 Williams PJ, Reeder M, Pekney NJ, Risk D, Osborne J, McCawley M. 2018.
518 Atmospheric impacts of a natural gas development within the urban context of
519 Morgantown, West Virginia. *Science of The Total Environment* 639:406-416.